

4

Anatomic and Histopathologic Characteristics of the Conductive Tissues of the Heart

Cristina Basso, Siew Yen Ho, Stefania Rizzo, and Gaetano Thiene

Abstract

The chapter deals with the anatomic and histopathologic characteristics of the Conductive Tissues of the Heart. In the first part, the authors treat the normal anatomy, histology and ultra-structural aspects of the conduction system, including the sinus node, the atrioventricular node and the internodal and interatrial myocardium with some historical notes on the discovery of these structures by early studies at the light microscope. In the second part, the pathological substrates of sino-atrial block, atrioventricular block, and ventricular preexcitation syndrome are extensively reviewed. Both congenital and acquired (inflammatory, degenerative, neoplastic, iatrogenic) diseases underlying conduction system disturbances are herein discussed in terms of gross and histological features.

Keywords

Anatomy • Anomalous pathways • Atrioventricular node • Bundle branches • Conduction system • Congenital heart diseases • His bundle • Histology • Sinus node • Internodal pathways

The cardiac conduction tissues in the human heart comprise specialised myocytes that can be differentiated from working myocardium with routine histological staining. They are located in specific regions of the heart to form

the sinus node and the atrioventricular (AV) node that then extends into the AV bundle and bundle branches. Both cardiac nodes are sited in the atria with working atrial myocardium in between (so called internodal preferential pathways) (Fig. 4.1). Atrial myocardium is separated from ventricular myocardium by fibro-fatty tissues at the AV junction and rings. In the normal heart, the continuation of specialised myocytes from the AV node that forms the bundle of His, penetrating the central fibrous body, is the only muscular continuity between atrial and ventricular myocardium, allowing atrial impulses to slow down in the AV node and to be conveyed to the ventricles in orderly fashion. In this chapter, we will deal with normal and pathologic features of the conductive tissue of the heart.

C. Basso, MD, PhD • S. Rizzo, MD
G. Thiene, MD, FRCP Hon. (✉)
Pathological Anatomy, Department of Cardiac,
Thoracic and Vascular Sciences,
University of Padua Medical School,
Via A. Gabelli, 61, 35121 Padova, Italy
e-mail: cristina.basso@unipd.it;
stafania.rizzo@studenti.unipd.it;
gaetano.thiene@unipd.it

S. Y. Ho, PhD, FRCPath
Cardiac Morphology Unit, Children's Services,
Royal Brompton Hospital, London SW3 6NP, UK
e-mail: yen.ho@imperial.ac.uk

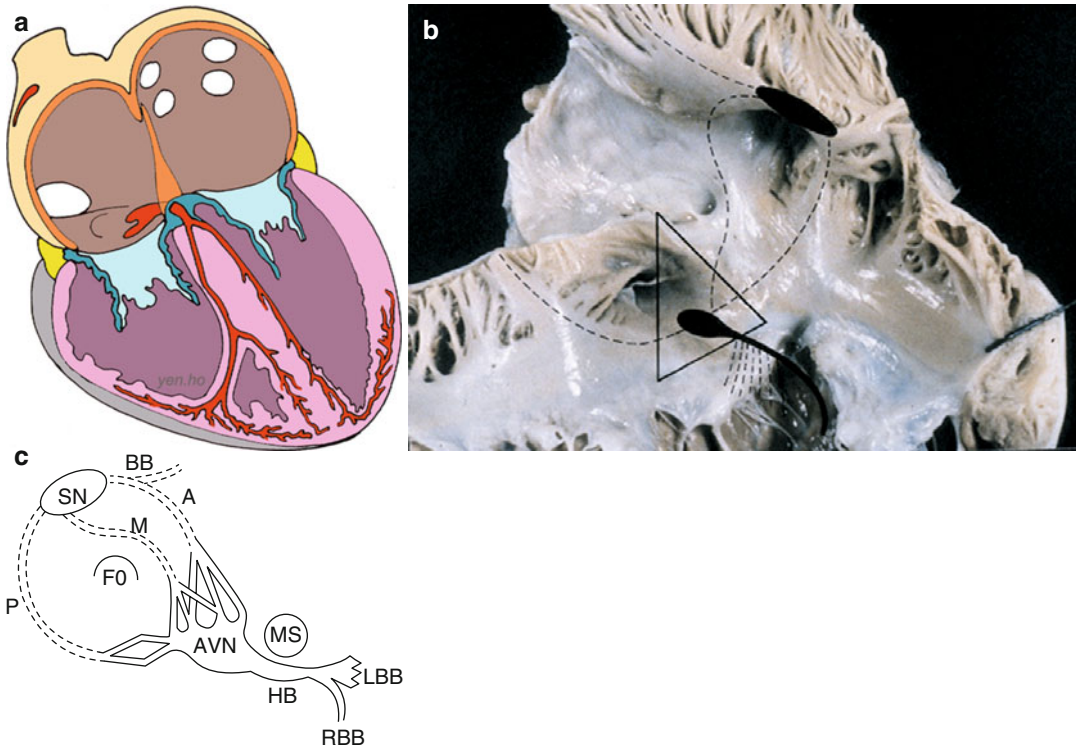


FIGURE 4–1. (a) Diagram illustrating the topography of the specialised conduction system (red) of the heart; (b) view of the right atrium: the sinus node is located at the root of the superior vena cava, lying over the crista terminalis, and the AV node within the triangle of Koch. Dotted lines depict internodal pathways and left bundle branch. (c) Diagram

illustrating the internodal pathways (A anterior, M middle, P posterior) between the sinus node (SN) and the AV node (AVN) and the interatrial connection through the so-called Backman's bundle (BB). FO fossa ovalis, MS membranous septum, HB His bundle, LBB left bundle branch, RBB right bundle branch

Normal Anatomy

Sinus Node: Location, Anatomy and Histology

Discovered by Keith and Flack a century ago [1], the sinus node (the cardiac pace-maker) was illustrated as lying in the terminal groove (sulcus terminalis), in the lateral part of the junction between the superior vena cava and the right atrium (see Fig. 4.1). The original description reports that “*there is a remarkable remnant of primitive fibres persisting at the sino-auricular junction in all the mammalian hearts examined. These fibers are in close connection with the vagus and the sympathetic nerves, and have a special arterial supply; in them the dominating rhythm of the heart is believed to normally arise*” [1].

This lateral position was endorsed by Koch [2] and by most subsequent investigators [3–5].

A horse-shoe arrangement with the node situated anteriorly and draped over the crest of the atrial appendage as described by Hudson [6] is found in approximately 10 % of hearts [7].

The shape of the node, more commonly, is like a tadpole with a head section situated antero-superiorly and a tapering tail that extends for a variable distance inferiorly toward the entrance of the inferior vena cava (see Fig. 4.1) [2, 8]. In the subepicardium, the long axis of the node is parallel to the terminal groove, but the body and tail then penetrate intramyocardially towards the subendocardium. Thus, the fatty tissues of the terminal groove serves as the epicardial landmark whereas the terminal crest (crista terminalis) in the antero-lateral quadrant of the entrance of the superior vena cava is the endocardial landmark for the nodal head. The nodal body and tail lie in the terminal crest and are at varying depths from the endocardium [8]. In the adult the length

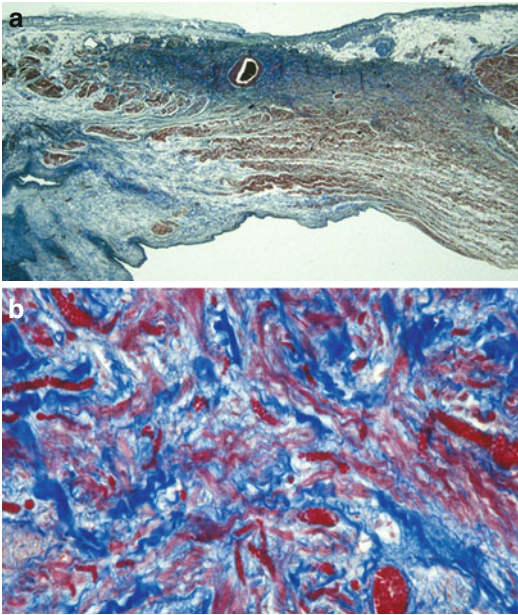


FIGURE 4–2. (a) Longitudinal section of the sulcus and crista terminalis: the sinus node is located sub-epicardially and centered by the sinus node artery. Note the abundant extracellular matrix (Heidenhain trichrome $\times 5$); (b) at higher magnification, the small, interlacing pale myocytes with P and T cells are visible (Heidenhain trichrome $\times 40$)

of the nodal body is approximately 1–2 cm but the tail portion can extend considerably longer.

The artery supplying the node is a branch from the proximal right coronary artery in 55 % of hearts and from the left circumflex coronary artery in the remainder [7]. The nodal artery approaches the node from anteriorly in majority of hearts but can also approach from posteriorly or form an arterial circle around the cavo-atrial junction [9]. Typically, the nodal artery passes centrally through the length of the nodal body.

The node is a specialised muscular structure composed mainly of small, interlacing myocytes of no definite orientation within a background of extracellular matrix, surrounded by parasympathetic ganglionated plexus accounting for nerve supply [10]. On histology, the node appears as a dense aggregation and the specialised myocytes (P cells) appear less darkly stained than the neighboring working atrial myocardium (Fig. 4.2). These P cells have pacemaker activity due to spontaneous depolarization. At electron microscopy, P cells typically occur in small clusters of 3 or 4, surrounded by

a basement membrane and contain very simple intercellular junctions (Fig. 4.3). The intercellular junctions of the P cells are composed mainly of undifferentiated regions, with only a few desmosomes and even more rarely, a very small gap (nexus).

However, the nodal margins may be discrete with fibrous separation from atrial myocardium or interdigitate through a transitional zone. In the latter, prongs of nodal (P) and transitional (T) cells extend into the atrial myocardium but actual cell-to-cell contact is uncertain. Prongs radiating from the nodal body are common [8]. Occasional prongs can be found extending toward the wall of the superior vena cava. In some hearts, the distal part of the nodal tail appears as clusters of specialised myocytes amongst fibrofatty tissues and atrial myocytes in the subendocardium [8].

Internodal and Interatrial Myocardium

The transmission of the cardiac impulse from the sinus node to the AV node is often depicted as through three internodal tracts in Cardiology texts. These are portrayed as cable-like structures that pass anteriorly, medially and posteriorly in the right atrium (Fig. 4.1b, c). However, light microscopy and electron microscopy examinations have not revealed discrete specialised bundles in the atrial walls that could satisfy the criteria of conduction tissue tracts. Apart from the occasional caudal extension of the sinus node into the crista terminalis, there are no histologically recognizable specialised pathways. This is also true for the interatrial conduction through the so-called Backman's bundle [11]. Instead, the walls of the atria are made up of broad bands of working myocardium that are separated by orifices of the veins, foramen ovale, and the AV valves. Parts of the wall, for example the crista terminalis and the anterior rim around the foramen ovale, show a better alignment of the myocytes than other parts, allowing preferential propagation of the cardiac impulse. Thus, the spread of excitation from pacemaker to AV node as well as to the left atrium is along broad wavefronts in these muscular bands. Through its transitional cell zone, the AV node acts as the 'receiver' that then

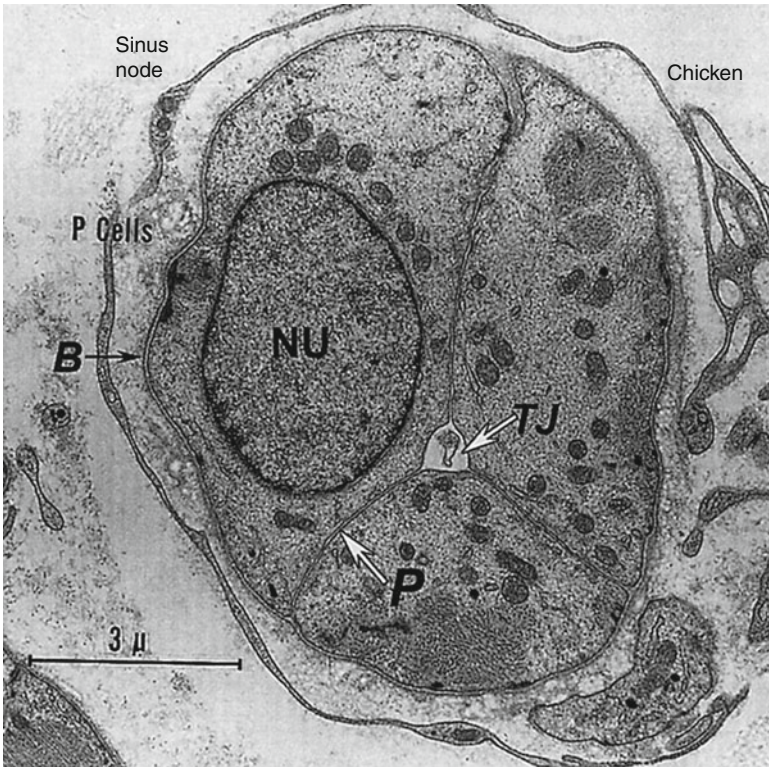


FIGURE 4–3. Clusters of P-cells in the chicken sinus node. Note a basement membrane (*B*) surrounding the entire P-cell cluster. Junctions between the three P cells here are composed entirely of “undifferentiated regions,” with simple apposition of plasma membranes (*P*) at a constant distance from each other (*TJ* triadic junction, *NU* nucleus) (From James [10]. Reprinted with permission from Elsevier Limited)

channels the impulse to the ventricles via the specialised conduction bundle and bundle branches.

AV Conduction System: Location, Anatomy and Histology

The pioneering work of Tawara [12] a century ago likened the AV system to a tree, with its roots in the atrial septum, and its branches ramifying within the ventricles. He recognized a collection of histologically distinct cells at the base of the atrial septum that he termed the “knoten”, and that has subsequently become known as the AV node.

Being the atrial component of the AV conduction system, the AV node receives, slows down and conveys atrial impulses to the ventricles. It is an interatrial structure located on the right side of the central fibrous body and when considered from the right atrial aspect it is situated within the triangle of Koch (see Fig. 4.1). The triangle described by Koch [2] is bordered anteriorly by the ‘annulus’ of the septal leaflet of the tricuspid valve, posteriorly by the tendon of Todaro that

runs within the sinus septum (Eustachian ridge or crista dividens), and inferiorly by the orifice of the coronary sinus and the atrial vestibule (see Fig. 4.1). The vestibule is recognised by arrhythmologists as the so-called ‘septal isthmus’. This is the target for ablating the slow pathway in patients with AV nodal reentrant tachycardia [13]. The central fibrous body itself is comprised of a thickened area of fibrous continuity between the leaflets of the mitral and aortic valves, termed the right fibrous trigone (Fig. 4.4), together with the membranous component of the cardiac septum. The tendon of Todaro inserts into the central fibrous body that lies at the apex of the triangle (Fig. 4.5) [14]. The ‘annulus’ of the septal leaflet of the tricuspid valve crosses the membranous septum (Fig. 4.6a).

In the original description by Tawara, it is reported that “*the system is a closed muscle bundle that resembles a tree, having a beginning, or root, and branches... The system connects with the ordinary ventricular musculature for the first time at the terminal ramifications*” [12]. Moreover, in 1893 His was the first to observe the bundle as

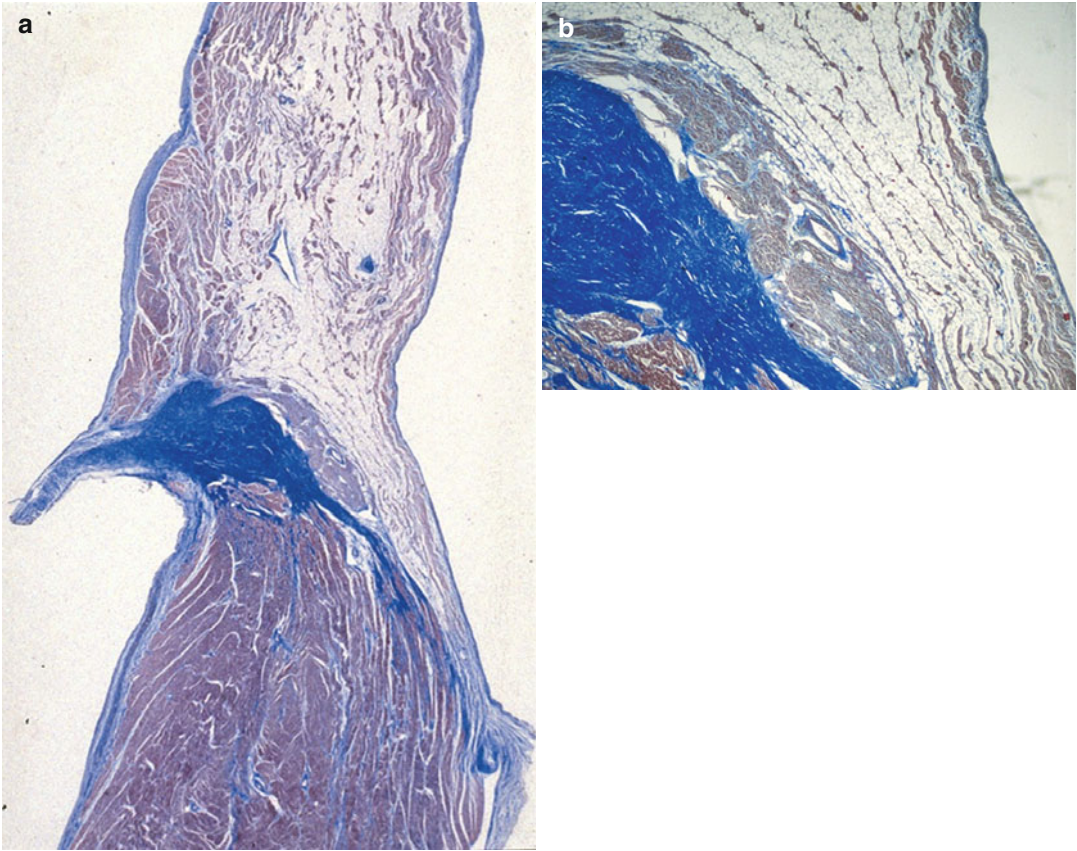


FIGURE 4-4. (a) The AV node is located on the right side of the central fibrous body, which extends to the fibrous mitro-aortic continuity (Heidenhain trichrome $\times 3$); (b) close-up of the AV node, with compact

and transitional zones, centered by the AV nodal artery (Heidenhain trichrome $\times 12$)

follow: “ I have succeeded in finding a muscle bundle which unites the auricular and ventricular septal walls...The bundle arises from the posterior wall of the right auricle near the auricular septum, in the atrioventricular groove; attaches itself along the upper margin of the ventricular septal muscle...proceeds on top of this toward the frontal until near the aorta it forks itself into a right and left limb” [15].

The compact node, approximately 5 mm long, 5 mm wide and 0.8 mm thick in adults [16], is adjacent to the central fibrous body on the right side but is uninsulated by fibrous tissue on its other sides, allowing contiguity with atrial myocardium (see Fig. 4.4). Owing to the lower level of attachment of the tricuspid valve relative to the mitral valve, the AV node ‘leans’ toward the right atrial side and is a few millimetres far from the endocardium (see Fig. 4.4).

From the node extends the AV bundle of His that passes through the fibrous core of the central fibrous body (see Fig. 4.5). The bundle veers leftward as it penetrates the central fibrous body, taking it away from the right atrial endocardium and toward the ventricular septum. In majority of hearts it emerges to the left of the ventricular septal crest but is insulated from ventricular myocardium by fibrous tissue and from atrial myocardium by the membranous septum itself (Fig. 4.6b). Viewed from the left ventricle, the landmark for the AV bundle is the area of fibrous continuity between aortic and mitral valves that is adjacent to the membranous septum. Viewed from the aorta, the interleaflet fibrous triangle between the right and the non-coronary sinuses adjoins the membranous septum and the AV bundle passes beneath that part of the septum (Fig. 4.7).

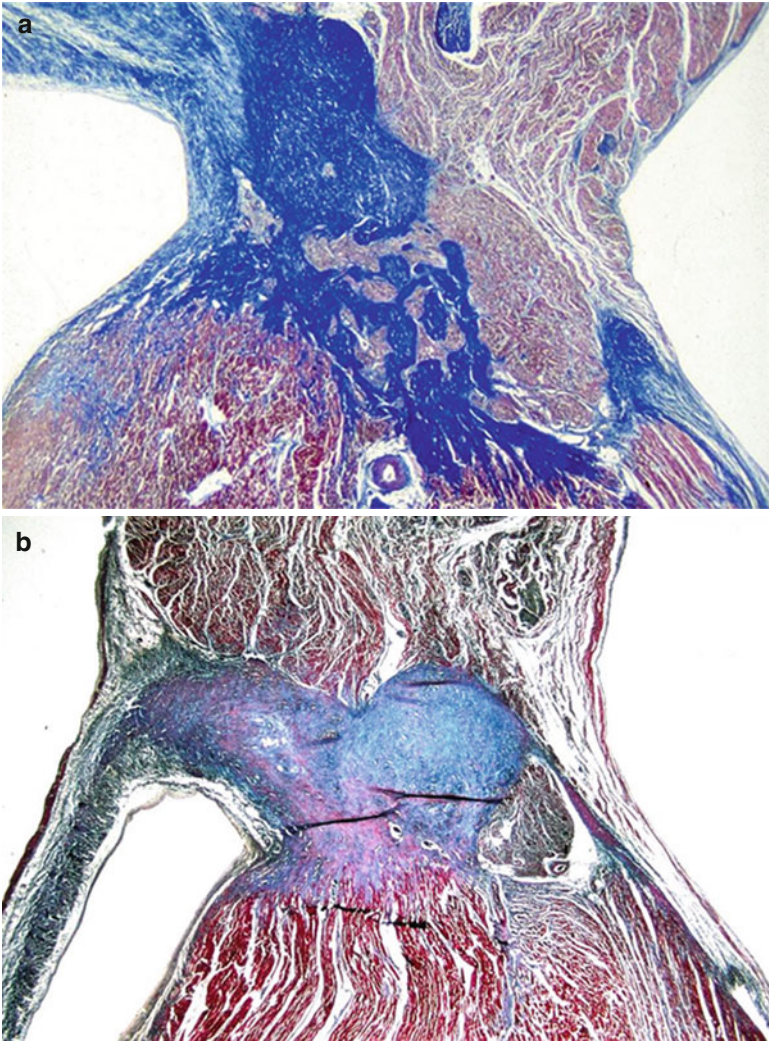


FIGURE 4–5. (a) Penetrating AV bundle: note on the top the tendon of Todaro, approximating the central fibrous body (Heidenhain trichrome $\times 12$); (b) common AV bundle running within the fibrous body on the right side and surrounded by a fibrous sheath (Heidenhain trichrome $\times 12$)

Progressing forward, the AV bundle divides into left and right bundle branches, still ensheathed by fibrous tissue until the bundle branches have descended approximately half-way down the septum. Descending in the subendocardium, the left bundle branch fans out into interconnecting fascicles as depicted in the original drawings by Tawara [12]. The fascicles then ramify into thinner and thinner strands toward the apex. Sometimes its proximal subendocardial course is visible due to the glistening sheen of its fibrous sheath. Owing to its fan-shape, its proximal portion is considerably more extensive than that of the right bundle branch. The right bundle branch, a cord-like structure, is a direct continuation of the AV bundle. In majority of hearts, since the AV bundle is usually to

the left of the ventricular septal crest instead of being astride the crest, the right bundle branch passes through the septal myocardium before reaching the subendocardium of the right side of the ventricular septum (Fig. 4.6). The anatomical landmark for its emergence is the base of the medial papillary muscle (Lancisi muscle). From there its proximal portion can often be seen as a white line in the subendocardium of the septomarginal trabeculation where it is still within a fibrous sheath. Distally, ramifications of the right bundle branch extend to the apex of the heart, and are also carried across the ventricular cavity through the moderator band and other muscular bundles (see Fig. 4.1). In some hearts, an additional bundle arises from the branching bundle, in between the bundle

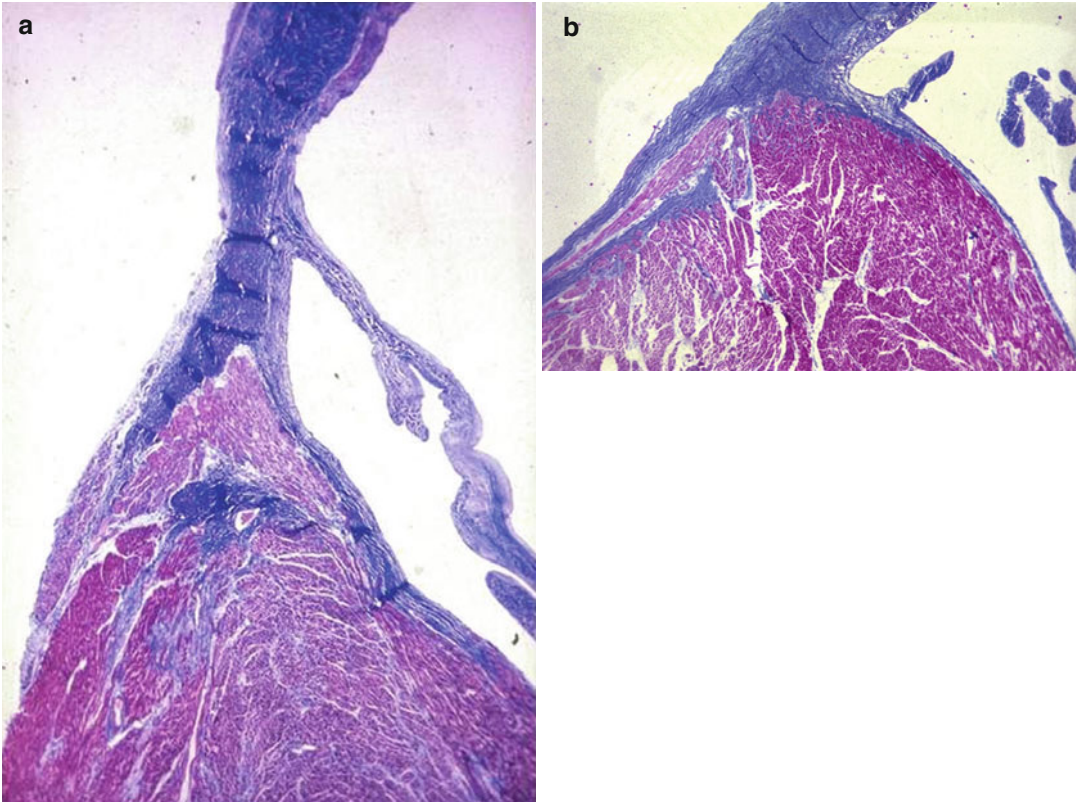


FIGURE 4–6. (a) Bifurcating bundle astride the ventricular septal crest, underneath the membranous septum: note the insertion of the septal leaflet of the tricuspid valve dividing the membranous septum in interventricular and AV components (Heidenhain trichrome $\times 4$);

(b) Course of the bifurcating bundle on the left side of the ventricular septal crest: note the insulation of the bundle by fibrous tissue and the intramyocardial course of the proximal right bundle branch (Heidenhain trichrome $\times 8$)

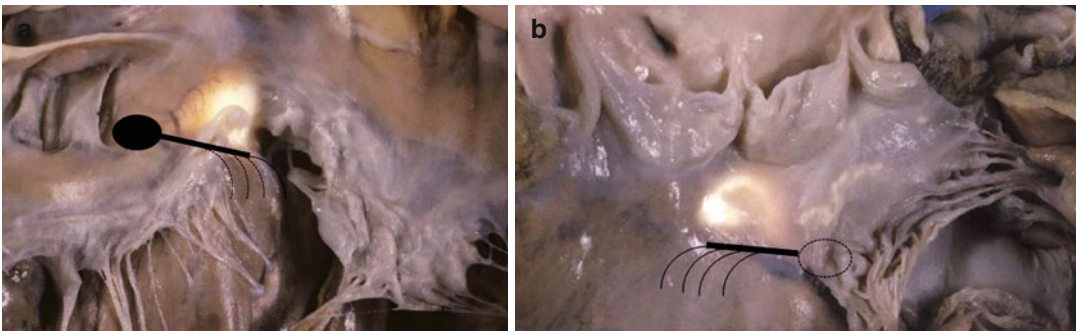


FIGURE 4–7. The “core” of the heart in correspondence of the membranous septum, where the specialised AV junction is located (a, right side view; b, left side view). The landmark of the AV bundle from the left side

is the continuity between the aortic and mitral valve, adjacent to the membranous septum, which is located underneath the interleaflet triangle between the right and posterior non-coronary cusps

branches, and extends forward. This is described as the ‘dead end tract’ and is more often seen in fetal and infantile hearts than in adult hearts [17]. It continues from the main bundle antero-superiorly toward the root of the aorta.

Under the microscope, the specialised AV conduction bundle and its main branches are readily identifiable by their encasing fibrous sheaths using basic histological stains. In keeping with Tawara’s work [12], it is the continuity from

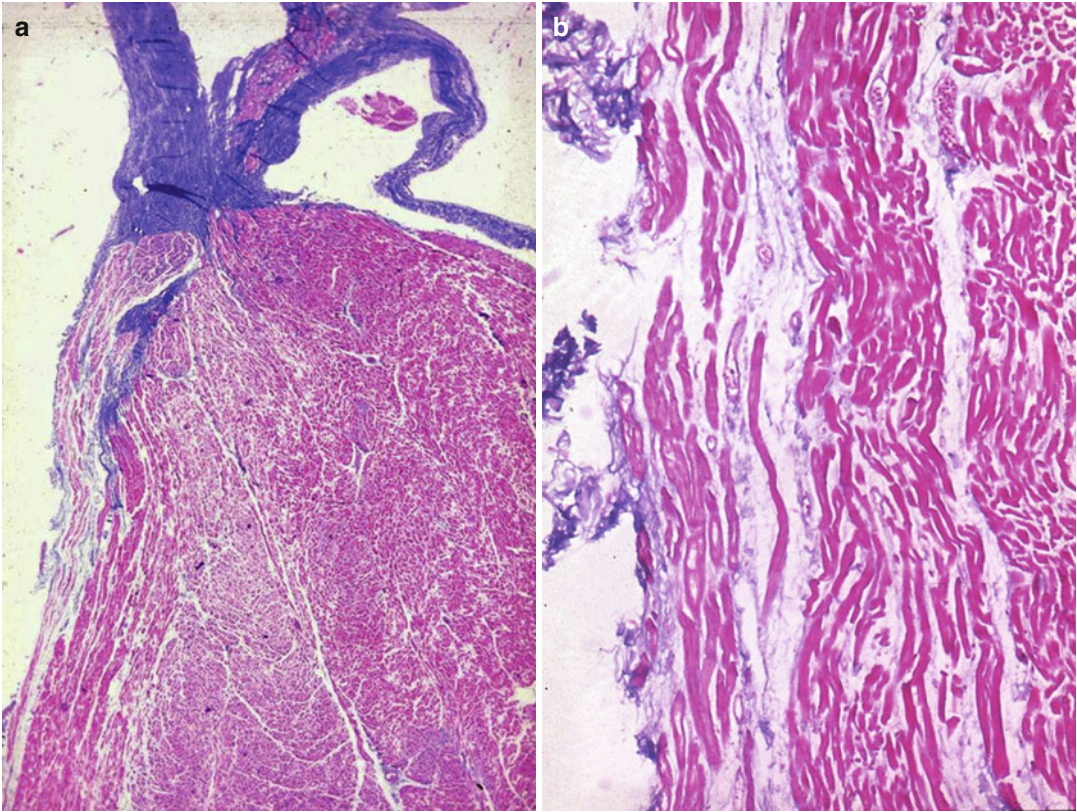


FIGURE 4–8. (a) The course of the left bundle branch under the subendocardium of the left side of the ventricular septum (Heidenhain trichrome $\times 5$); (b) Close-up of the Purkinje-like cells of the left bundle branch (Heidenhain trichrome $\times 25$)

section to section that serves as the most reliable method for histological localisation of the AV conduction system. Beginning with the AV node, which has the inherent function of delaying the cardiac impulse, the human node has a compact portion, and zones of transitional cells (see Fig. 4.4). The compact node is recognizable, when seen in cross-sections, as a half-moon shaped structure hugging the central fibrous body. The nodal cells are smaller than atrial myocytes. Like the cells of the sinus node, the compact nodal cells are closely grouped, and frequently arranged in interweaving fashion. In many hearts, the compact node has a stratified appearance with a deep layer overlain by a superficial layer. When traced inferiorly, toward the base of Koch's triangle, the compact area separates into two prongs, usually with the artery supplying the node running in between. The prongs bifurcate toward the tricuspid and mitral annuli respectively. Their lengths vary from heart to heart and in recent years the rightward prongs have been

implicated in so-called slow pathway conduction in AV nodal re-entrant tachycardia [18]. Interposing between the compact node and the working atrial myocardium is a zone of transitional cells (see Fig. 4.4b). These cells are histologically distinct from both the cells of the compact node and the working cells of the atrial myocardium, and are not insulated from the surrounding myocardium. The cells are long, attenuated, and have a wavy appearance. They tend to be separated from one another by thin fibrous strands. According to established definitions, transitional cells do not represent conducting tracts but they provide the crucial bridge between the working and the specialised myocardium. Transitional cells interpose between the left and right margins of the compact node and the myocardium from the left and right sides of the atrial septum. Wider extensions of transitional cells are present inferiorly and posteriorly between the compact node and the mouth of the coronary sinus and into the Eustachian ridge. The right

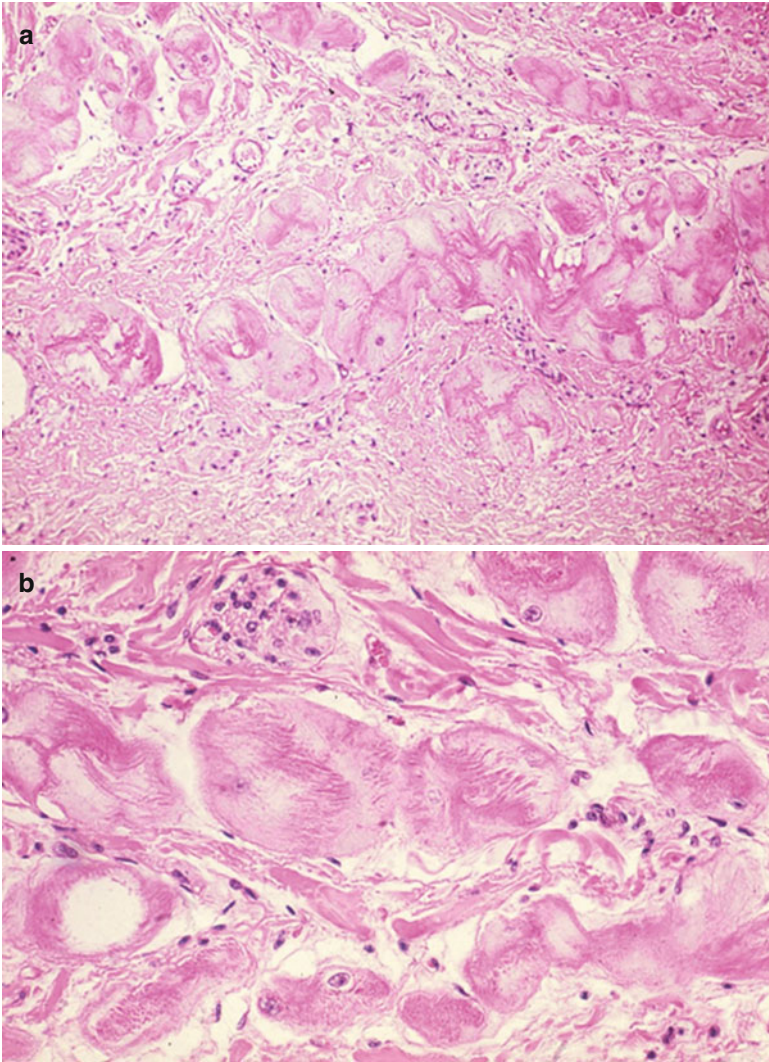


FIGURE 4–9. Purkinje cells in ungulates' heart. **(a)** Large, swollen and pale specialised cardiac myocytes as compared to the surrounding working myocardium (haematoxylin-eosin $\times 40$); **(b)** Purkinje cells at higher magnification (haematoxylin-eosin $\times 120$)

margin of the node faces the vestibule of the right atrium. Here, an overlay of working myocytes in the subendocardium from the atrial wall in front of the fossa ovalis streams over the layer of transitional cells.

When the conduction system is followed distally from the compact node into the penetrating bundle of His, there can be little difference in the cellular composition in the two areas. The specialised cells themselves, however, become aligned in a more parallel fashion distally. Even so, Tawara [12] proposed that the distinction be made on purely anatomical grounds. The key change from node to bundle is that the bundle is insulated by fibrous tissue from the adjacent myocardium (see Fig. 4.6b), preventing atrial

activity from bypassing the node. Thus, all atrial activity must be channeled via the AV node.

Being surrounded by fibrous tissue, the penetrating bundle is the first part of the axis which qualifies as a conducting tract (see Fig. 4.5b). The cells are marginally larger than compact nodal cells and they increase in size as the penetrating bundle continues into the AV bundle and branching bundle (Fig. 4.8). Here, the cells are very similar in size to ventricular myocytes. Swollen cells or Purkinje cells are not characteristic of specialised myocytes in the human heart and are seldom seen. However, they are typically seen in ungulates (Fig. 4.9) [12, 19, 20]. The AV bundle, branching bundle and proximal parts of the bundle branches are recognizable by the fibrous

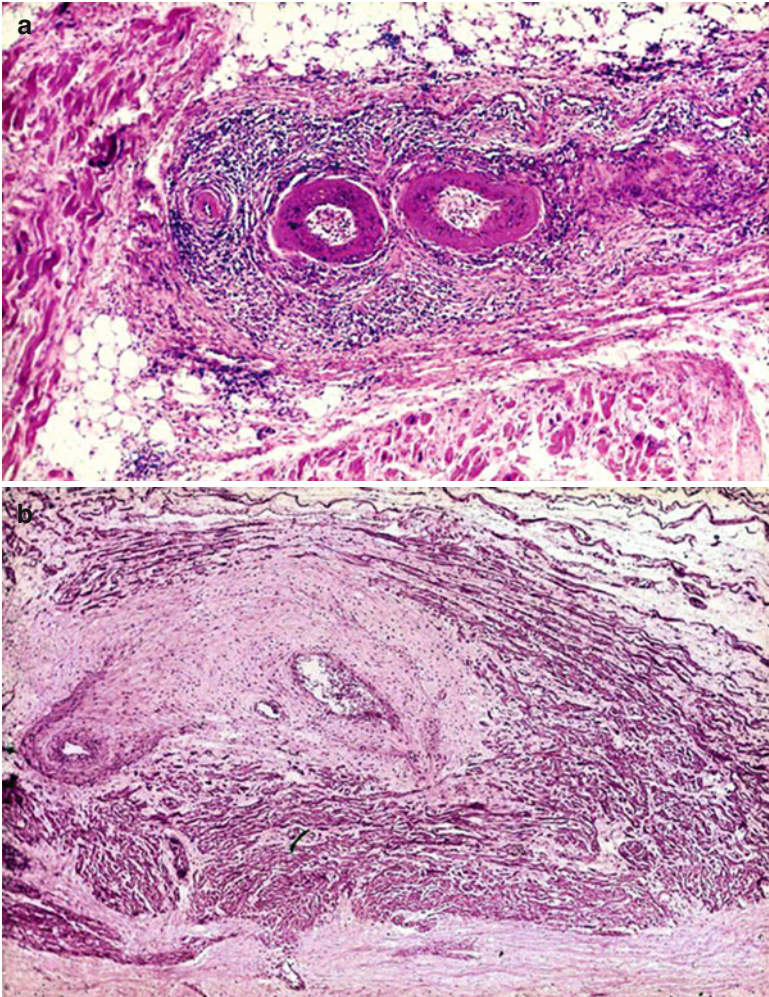


FIGURE 4–10. (a) Arteritis of the sinus node artery in polyarteritis nodosa: note the inflammation extended to the nodal specialised myocardium (haematoxylin-eosin $\times 15$); (b) AV node in polyarteritis nodosa: the AV nodal artery shows aneurysm and recanalized thrombus with extensive fibrotic replacement of conductive cells (haematoxylin-eosin $\times 15$)

sheaths that encase them, insulating them from the adjacent working ventricular myocardium. When the bundles lose their fibrous sheaths distally, it is no longer possible to distinguish conduction tissues from working myocardium.

Pathology

Sino-Atrial Block and Sinus Arrest

The atrial activation may be impaired (atrial standstill) for two main reasons: impulses are not generated from the sinus node (sinus arrest) or their propagation to the atria is impeded (sinus block). In the etiology of

sino-atrial block, several lesions of the sinus node and its innervation have been described, besides neurovegetative changes (vagal stimulation), drug sensitivity – intoxication and hyperkalemia.

From the pathological viewpoint, abnormalities of the sinus node artery, of the specialised myocardium of the sinus node and/or of its connections with the atrial myocardium (nodal approaches), and of the nodal ganglionated plexus have been reported. Myocardial infarction due to occlusion of the right coronary artery, proximal to the origin of the sinus node artery, remains the main cause of sinus node dysfunction, causing severe damage of the node and its atrial approaches in terms of necrosis, leukocytic

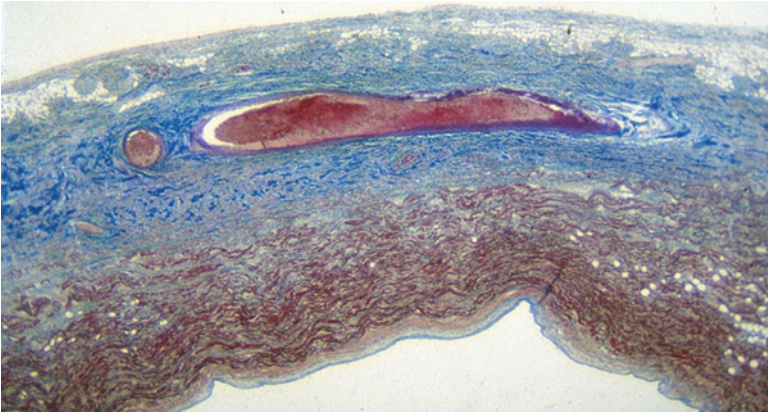


FIGURE 4–11. Massive infarction of the sinus node and crista terminalis by occlusive thromboembolism of the nodal artery (Heidenhain trichrome $\times 6$)

infiltrates and haemorrhage. Sinus node artery perfusion can be also altered as a consequence of arteritis (Fig. 4.10) and embolism (Fig. 4.11), amyloid deposition and connective tissue disorders [21–25]. Recipient sinus node in cardiac transplantation undergoes to massive infarction due to nodal artery transection during surgical procedure and the donor sinus node artery may show obstructive intimal proliferations due to allograft vasculopathy (chronic rejection) (Fig. 4.12) [26].

AV Block

Any disease, either acute or chronic, that affects the myocardium may produce AV block, which may occur at the level of AV node approaches, AV node itself, penetrating or branching part of the bundle, and bundle branches [21–23, 27].

Morgagni, Adams and Stokes share the merit of having individuated the clinical entity of AV block and, after the recognition of the anatomic basis of the AV conduction axis by His and Tawara, Mahaim did the first clinico-pathologic assessment of this entity [28].

Pathologically, AV block may be classified as being caused by congenital or acquired diseases [27]. As far as the *congenital* AV block in an otherwise normally developed heart, this is usually a benign condition, mainly due to a lack of connection between the atria and the peripheral conduction system, with fatty replacement of the AV node and nodal approaches [29]. Moreover, the AV bundle may present marked

fragmentation and septation. Maternal lupus with an immune mechanism plays a major etiopathogenetic role [30, 31].

Acquired AV block may be caused by *acute myocardial ischemia or infarction*. Inferior myocardial infarction may be complicated by third-degree AV block due to ischemic injury of the AV node itself. In particular, in postero-septal myocardial infarction, due to right coronary artery thrombotic occlusion in right dominant pattern, ischemic damage may involve atrial approaches to the AV node, AV node and His bundle. However, since the conducting tissues are resistant to ischemia, pathologic changes may be reversible and the AV block transient. Anterior myocardial infarction usually is associated with third-degree block due to ischemia or infarction of bundle branches; the branching bundle and bundle branches are often involved by the necrotic process, and by inflammatory infiltrates of the surrounding working ventricular myocardium [32]. Chronic ischemic heart disease, with or without infarction, may also be characterized by AV block, due to fibrotic changes of the bifurcating bundle and bundle branches, as well as of the crest of the ventricular septum [27].

The heart may be the target of *angioitides and collagen diseases*. Polyarteritis nodosa is a medium-large vessel vasculitis, with cardiac involvement in up to 80 % of cases. It typically manifests as pericarditis, coronary arteritis, myocardial infarction, arrhythmias and conduction disturbances [24]. Nodal arteries may be of

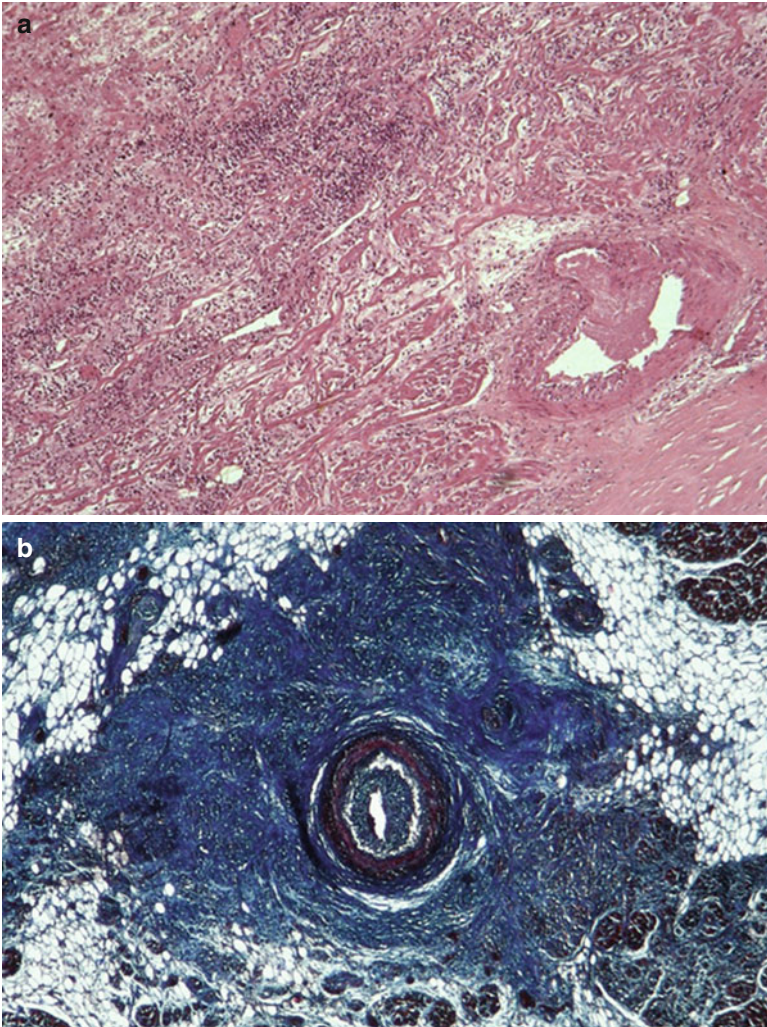


FIGURE 4–12. Conduction system pathology in the transplanted heart. (a) AV node shows severe acute rejection and thrombosis of the AV node artery (haematoxylin-eosin stain, original magnification a $\times 60$); (b) Histologic section of the donor sinus node artery in a patient with allograft vasculopathy (chronic rejection) who died 1,996 days after cardiac transplantation: note the obstructive, concentric intimal proliferation (Trichrome Heidenhain stain $\times 30$)

the proper size to be affected and the surrounding conductive tissue involved as well (Fig. 4.10b).

Cardiac involvement has been reported in 8–44 % of cases of Wegener’s granulomatosis. It typically manifests as pericarditis, coronary arteritis and myocarditis with granulomas involving the conduction system.

Similarly, cardiac involvement is seen in up to 70 % of cases of systemic lupus erythematosus. The most common findings are pericarditis, myocarditis, and Libman-Sacks endocarditis. As previously mentioned, congenital heart block is a peculiar feature of neonatal lupus syndrome, which is associated with transplacental transfer of anti-Ro and anti-La antibodies [30, 31]. In rheumatoid arthritis, rheumatoid granulomas

may affect the myocardium, endocardium, and valves as well as the conductive tissues; conduction disturbances and heart block have been reported [33].

Myotonic dystrophy, particularly type 1 myotonic dystrophy (Steinert’s disease), which is the commonest muscular dystrophy in adults, is characterized by myotonia, muscle weakness and a variety of other symptoms. Cardiac involvement is a frequent manifestation, the most prominent feature being conduction disturbances and arrhythmias, at risk of sudden death [34].

Myocarditis, especially in the acute phase, may present with AV block. It is usually transient and relates to inflammatory infiltrates and

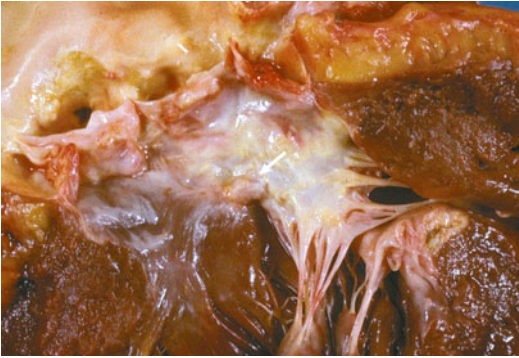


FIGURE 4-13. Calcific aortic valve stenosis with dystrophic calcification extended to the mitro-aortic continuity, where the His bundle is coming out

interstitial edema of the working myocardium surrounding the specialised conducting pathways, although involvement of the sinus node and AV node themselves have been reported. In *acute rheumatic carditis*, all the structures of the heart may be involved by the inflammatory process, conduction system included. In terms of rhythm disturbance, besides tachyarrhythmias, varying degrees of heart block, mostly first degree, are frequently recorded. Similar features with transient AV block may complicate *acute rejection* of the specialised conducting tissues themselves after cardiac transplantation (see Fig. 4.12) [26].

In *infective endocarditis* of the aortic and/or mitral valve, the inflammatory process may extend to the central fibrous body, thereby disrupting the AV node and His bundle as to produce AV block.

Complete AV block occurs also in the setting of *hypertensive heart disease*, and it can result from a combination of direct mechanical injury to the origin of the main left bundle branch at the crest of the ventricular septum and ischemic heart disease.

Calcific aortic stenosis has long been recognized as a cause of AV block, and many of the patients originally reported by Stokes correspond to this entity. The His bundle penetrates the central fibrous body in close proximity to both the aortic and mitral valve fibrous continuity, which is an usual site of dystrophic calcification, and extension of calcification can

directly involve the His bundle and/or the origin of the left bundle branch (Fig. 4.13).

Degenerative changes in the AV node or bundle branches are the most common cause of nonischemic AV block. The term *Lenègre-Lev syndrome* has been used to indicate an acquired complete heart block due to idiopathic fibrosis and calcification of the AV conduction system of the heart. However, we should keep distinct the two entities.

Lev disease is most commonly seen in the elderly, and is often described as senile degeneration of the conduction system [35]. It may imply, among others, degenerative changes at the summit of the ventricular septum, mitro-aortic fibrous continuity and membranous septum, consisting of fibrosis, hyalinisation, loss of conducting fibers, with or without calcification. The pathologic degenerative process, which has been traditionally considered the result of stress and strain, may affect mainly the branching bundle and the proximal right and left bundle branches. In the classical *Lev disease*, the origin of the left bundle branch and adjacent bifurcating bundle are destroyed with preservation of peripheral conduction system.

In contrast, AV block due to *Lenègre disease* occurs in younger people and the histopathologic features are in keeping with a primary myocardial disease that selectively destroys the right and left bundle branch conduction fibers, extending well down into the periphery (Fig. 4.14) [36]. It is a form of inherited cardiomyopathy confined in the specialised myocardium and should be classified among cardiomyopathies [37]. In 1999, *Lenègre disease* with AV block was linked to mutations of the *SCN5A* sodium channel gene, the same gene which may account also for congenital long QT syndrome type 3 and to *Brugada syndrome* [38].

Among *infiltrative myocardial diseases*, *sarcoidosis* is frequently associated with AV block due to *sarcoid granulomas* involving the specialised axis [39].

AV block may complicate aortic dissection when the dissecting haematoma infiltrates the atrial septum along with the retrograde extension, thus creating atrionodal discontinuity (Fig. 4.15) [40].

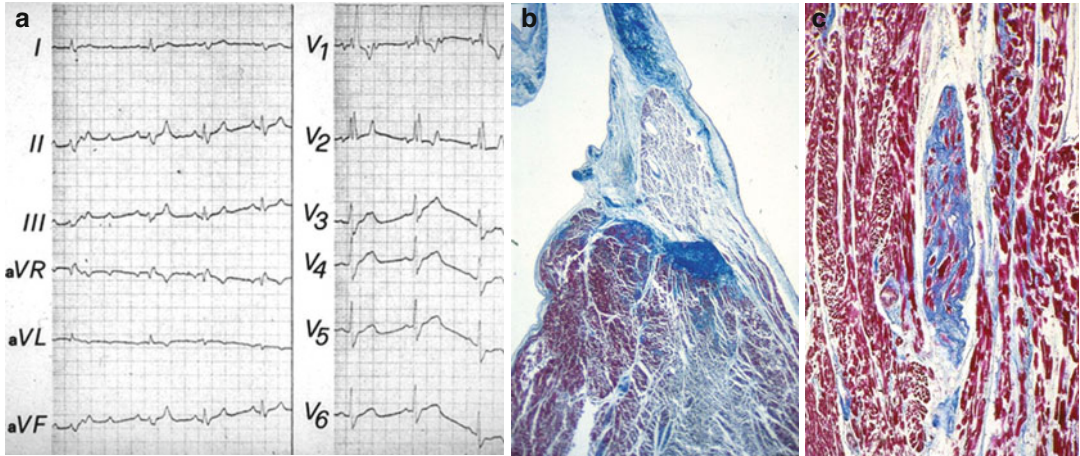


FIGURE 4–14. Lenègre disease with AV block. (a) 12 lead ECG tracing with intermittent AV block; (b) Sclero-atrophy of the origin of the left bundle branch from the His bundle (Heidenhain trichrome $\times 6$);

(c) Fibrotic interruption of the intramyocardial tract of the right bundle branch (Heidenhain trichrome $\times 60$)

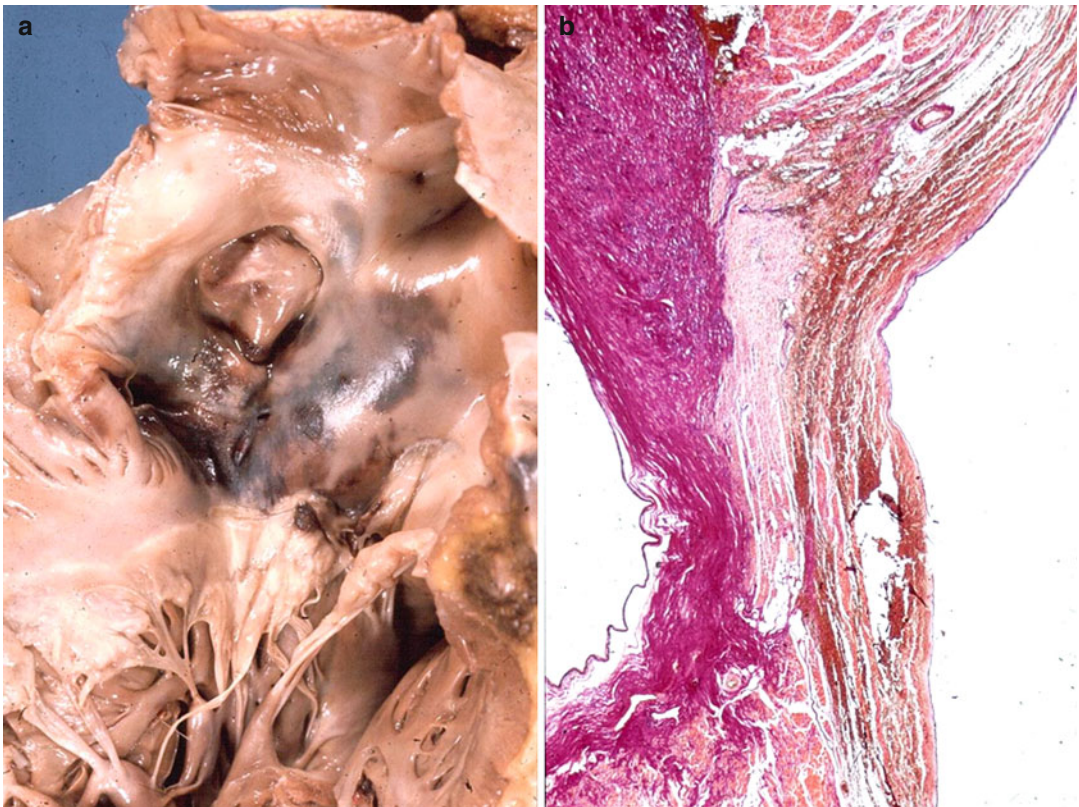


FIGURE 4–15. Type A aortic dissection with AV block. (a) Gross view of the interatrial septum with haemorrhage due to retrograde extension of dissecting haematoma seen from the right side; (b) At histology,

atrio-nodal discontinuity due to haemorrhagic infiltration of the interatrial septum and AV node atrial approaches (Heidenhain trichrome $\times 15$)

The term *celothelioma of the AV node*, known also as Tawarioma or cystic tumor of the AV node, refers to a tumor with heterotopic epithelial replacement of the AV node with

multicystic appearance (Fig. 4.16). It is a rare entity and, thus, an unusual cause of supra-His AV block, at risk of sudden death. Definitive histologic diagnosis is made at autopsy or in explanted hearts from cardiac transplantation [41, 42].

Complete AV block can appear in the setting of other *cardiac tumors*, including metastatic carcinoma of the heart, primary or secondary sarcoma and lymphoma, by direct infiltration or compression of the conducting tissue [43].

By studying a series of 177 cases with permanent AV block, Davies [27] showed that idiopathic bilateral bundle branch fibrosis is the commonest single cause (33 %), followed by ischaemic damage (17 %), cardiomyopathies (14 %) and calcific AV block (10 %). The remaining causes of chronic AV block were individually very rare ranging through tumour involvement, congenital defects, collagen diseases and surgical or traumatic damage.

As far as the site is concerned, according to Rossi [21] the frequency of AV block-producing lesions seems to increase in a downwards direction along the AV conducting pathway. Among 400 cases of AV block, which he studied by the serial section histological technique, the AV conduction discontinuity accounting for block could be ascribed to distal lesions of both bundle branches and/or bifurcating bundle in 60–70 % of cases, of the common His bundle in 15%, of the AV node in 10–14 % and of the atrio-AV nodal approaches in 5–11 % (Fig. 4.17).



FIGURE 4-16. Cystic tumor of the AV node: note the multicystic neoplasm at the level of the AV node (Heidenhain trichrome x5)

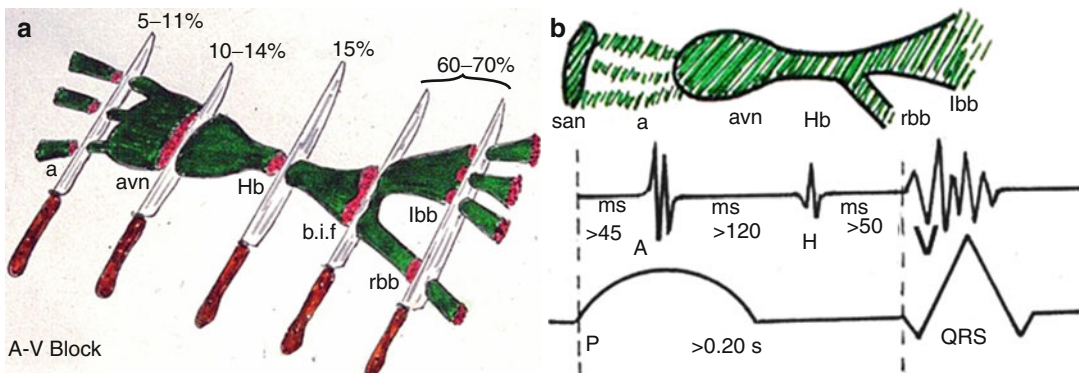


FIGURE 4-17. Site of AV blocking lesions: 60–70 % of the interruption of the AV conduction axis is located in the bifurcating proximal bundle branches, accounting for prolongation of HV interval

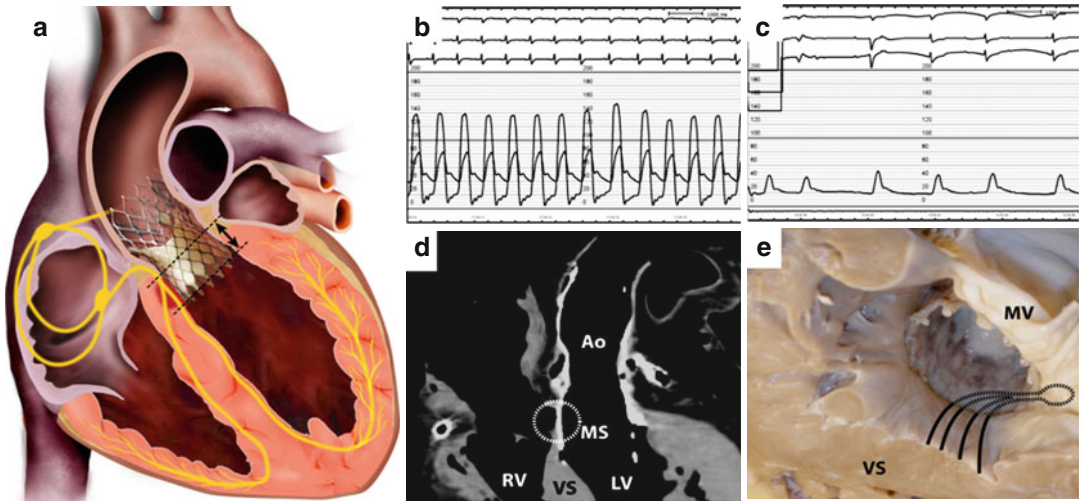


FIGURE 4–18. Iatrogenic AV block as a complication of transcatheter aortic valve implantation (TAVI) with CoreValve prosthesis. **(a)** Diagram illustrating anatomic relation between a deep prosthesis implantation into left ventricular outflow tract affecting electrical conduction system; **(b)** electrocardiogram showing right bundle branch block and 60 mmHg transaortic gradient at baseline. **(c)** electrocardiogram showing complete AV block immediately after TAVI. **(d)** computed tomography scan of heart explanted at autopsy showing the deep positioning of CoreValve

within left ventricular outflow tract, overlapping membranous septum (dotted circle) and crest of interventricular septum. **(e)** gross anatomic view of left ventricular outflow seen from below: the expansion of prosthesis frames in subaortic region compresses the ventricular septum and overlaps proximal branching of left bundle branch (dotted lines). Ao aorta, LV left ventricle, MS membranous septum, MV mitral valve, RV right ventricle, VS ventricular septum

Iatrogenic

AV block may occur following surgical or interventional manipulation of the conducting system. Surgical (aortic valve replacement, congenital septal defects repair, septal myectomy) or other therapeutic procedures (alcohol septal ablation in patients with obstructive hypertrophic cardiomyopathy, AV ablation in patients with supraventricular arrhythmias, and transcatheter aortic valve implantation) may be complicated by AV block [44–46]. In particular, in the setting of TAVI with prostheses protruding into the left ventricular outflow tract, independent predictors of pacemaker implantation are the depth of prosthesis implantation and pre-existing right bundle branch block (Fig. 4.18) [44]. Moreover, iatrogenic AV block with pacemaker implantation, may be a therapy of atrial fibrillation with high rate ventricular response. Electric (direct current-DC) or radiofrequency ablation of the AV node or His bundle may be selectively accomplished through the right atrium via the inferior vena cava, by delivering energy in the triangle of Koch at the level of the AV node or His bundle (Fig. 4.19).

The Conduction System in Congenital Heart Diseases

The site and course of the conduction system in congenital heart disease is related to the type of visceral symmetry, ventricular looping and septal defect.

In situs inversus with AV concordance the conduction system is located in a mirror image of the normal heart with sinus node on the left-sided morphologically right atrium.

In case of visceral symmetry, two sinus nodes are present in right atrial isomerism because of bilateral morphologically right atrium with two cristae terminalis, whereas no sinus node is present in left atrial isomerism since two morphologically left atria with no crista terminalis did develop. In the latter case the pacemaker activity is taken over by the AV node (Fig. 4.20) [47, 48].

In congenitally corrected transposition, with situs solitus and AV discordance (l-loop), the AV conduction system is located anteriorly, with an antero-lateral AV node giving rise to a His bundle penetrating the mitro-pulmonary fibrous

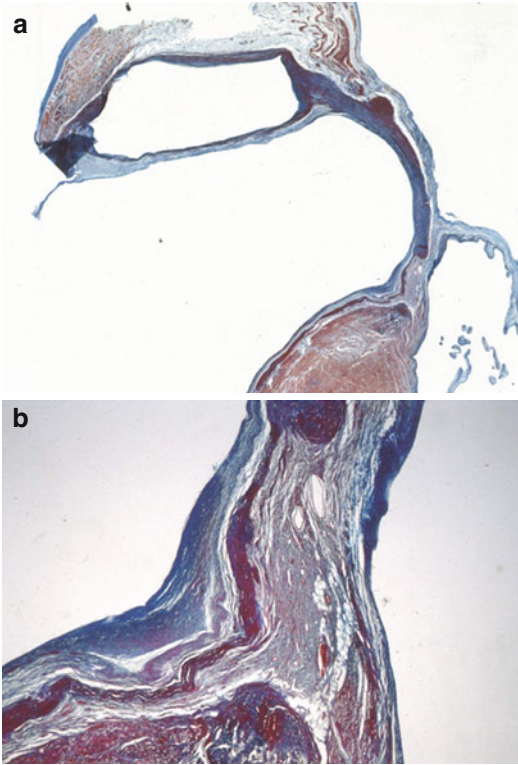


FIGURE 4-19. Ablation of the AV junction (iatrogenic AV block) to threat atrial fibrillation with high ventricular response. (a) At histology, the bifurcating bundle underneath the membranous septum appears interrupted by granulation tissue (Heidenhain trichrome $\times 5$). (b) Close up of the same (Heidenhain trichrome $\times 20$)

continuity and running anteriorly on the right-side of the ventricular septum, underneath the pulmonary valve (Fig. 4.21) [49]. In situs inversus with AV discordance (congenitally corrected transposition with situs inversus) the AV axis has been observed posteriorly, probably because of the d-loop in this setting [50].

In perimembranous ventricular septal defects, the His bundle and bifurcation are located in the postero-inferior rim, whatsoever the malformation (isolated VSD, tetralogy of Fallot, complete transposition of the great vessels, truncus arteriosus) (Figs. 4.22 and 4.23) [51]. They are at risk at the time of surgical closure if stitches are inserted in the infero-posterior rim (Fig. 4.24). A favorable condition is when the postero-inferior rim of the VSD is reinforced by the posterior limb of the trabecula septo-marginalis.

In AV canal, whether partial (ostium primum plus mitral cleft) or complete (common AV valve and orifice), the AV conduction axis is displaced well posteriorly and the penetration of the His bundle occurs at the postero-inferior rim of the huge AV septal defect; stitches in this site are at risk of AV block (Fig. 4.25) [52].

In valve malformation, the AV node may be located on the left side of the atrial septum, thus at risk of injury during mitral valve replacement [53].

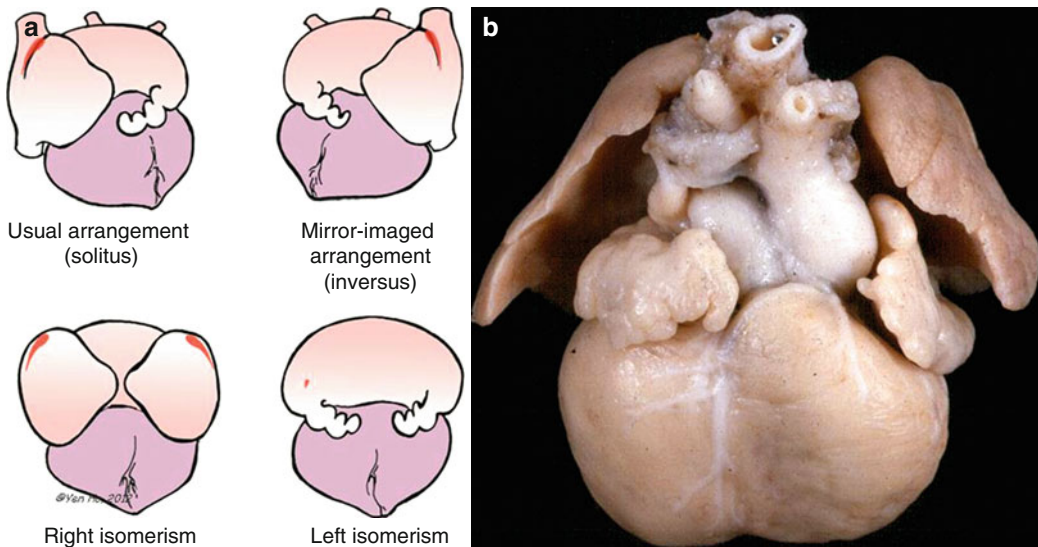


FIGURE 4-20. Site of the sinus node according to atrial symmetry. (a) Diagram illustrating the usual atrial arrangement (situs solitus), mirror-imaged arrangement (situs inversus), right isomerism and

left isomerism. (b) Gross view of a heart specimen with left atrial isomerism (note the two left auricular appendices) and absent sinus node

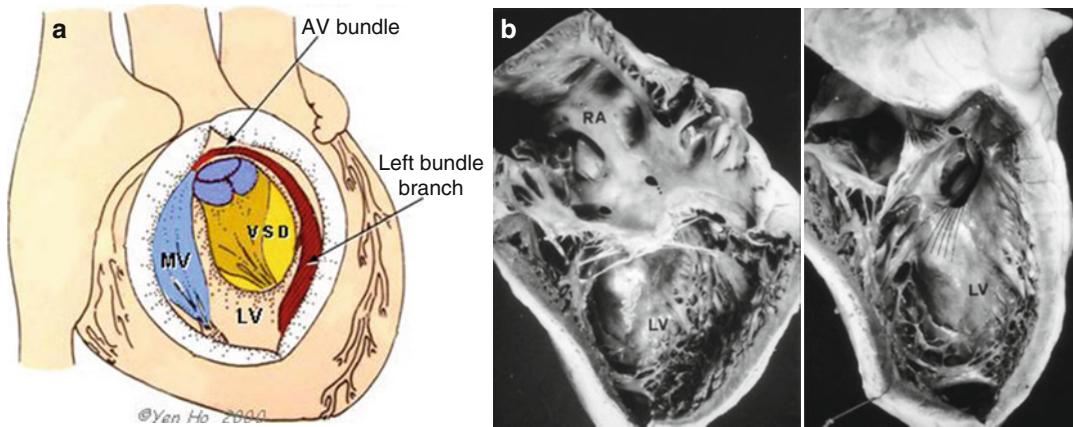


FIGURE 4–21. Conduction system in congenitally corrected transposition of the great arteries with situs solitus. (a) Diagram illustrating the AV conducting system displaced anteriorly. MV mitral valve, VSD ventricular septal defect; (b) gross view of the anatomical specimen

with atrioventricular discordance (right atrium–RA to left ventricle–LV) and ventriculo-arterial discordance (left ventricle–LV to pulmonary artery): note the anterior location of the AV conducting axis

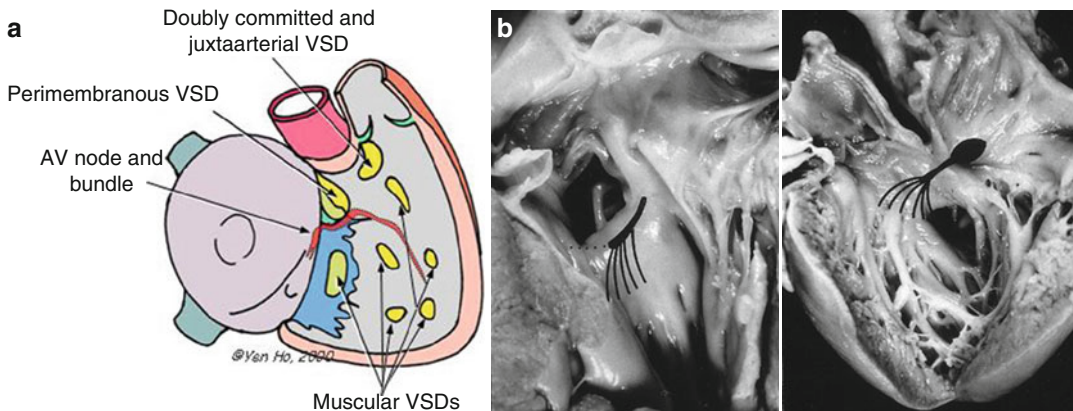


FIGURE 4–22. AV conduction system in ventricular septal defects (VSD). (a) Diagram illustrating the location of the AV conducting axis related to various types of VSD: doubly committed and juxtaarterial, perimembranous, muscular; (b) Gross view of heart specimens with perimembranous and muscular VSD: note the location of the AV node, bundle and left branch seen from the *left sides*

Ventricular Preexcitation and Enhanced AV Conduction

Accessory AV connections accounting for ventricular preexcitation may be “direct” (working to working myocardium) when located outside the specialised AV junction and connecting directly the atrial and ventricular myocardium (so-called “Kent fascicle”) or “mediated” (working to specialised myocardium or vice versa) when they involve the specialised AV junction

and connect either the septal atrial myocardium with the His bundle (James or Brechenmacher fibers) or the AV conduction axis with the ventricular myocardium (Mahaim fibers) [54].

A rare condition that promotes early ventricular excitation is the enhanced AV conduction (so-called Lown-Ganong-Levine syndrome [55]). The impulse runs very quickly through the AV node and His bundle, with a short PR interval and a normal QRS complex. Two histological backgrounds have been reported to

and connect either the septal atrial myocardium with the His bundle (James or Brechenmacher fibers) or the AV conduction axis with the ventricular myocardium (Mahaim fibers) [54].

A rare condition that promotes early ventricular excitation is the enhanced AV conduction (so-called Lown-Ganong-Levine syndrome [55]). The impulse runs very quickly through the AV node and His bundle, with a short PR interval and a normal QRS complex. Two histological backgrounds have been reported to

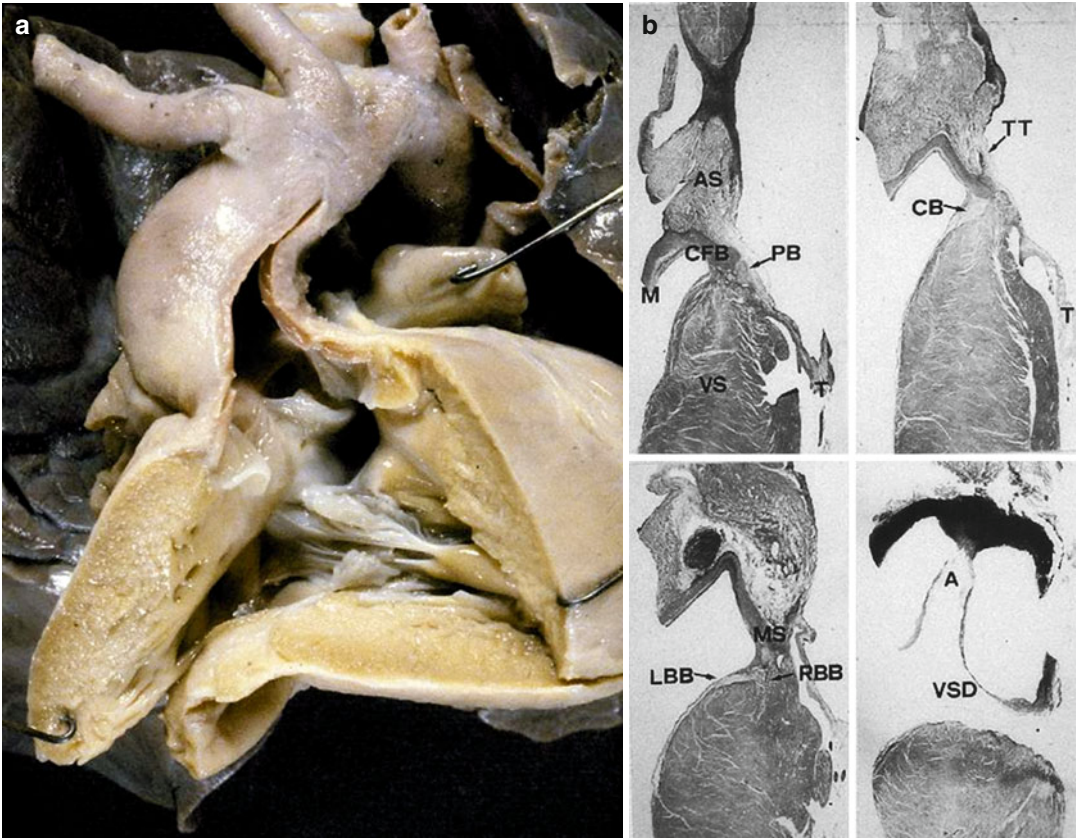


FIGURE 4–23. AV conduction system in tetralogy of Fallot. (a) Gross view of right ventricular outflows in a specimen with pulmonary atresia and perimembranous VSD; (b) At histology, note the course of common bundle (CB) and bifurcating bundle dividing into left and right branches

at the postero-inferior rim of the defect (A aorta, AS atrial septum, CFB central fibrous body, LBB left bundle branch, M mitral valve, MS membranous septum, PB penetrating bundle, RBB right bundle branch, T tricuspid valve, TT tendon of Todaro, VS ventricular septum)

explain the missed delay at the specialised AV junction: (a) a congenitally hypoplastic AV node, with a lessened bulk of specialised tissue to slow down impulse transmission from atria to ventricles (Fig. 4.26) [56]; (b) the presence of an atrio-His bundle of working myocardium that bypasses the AV node and transmits the activation signal directly to the His bundle without any delay at the nodal level. In both substrates, the onset of atrial fibrillation, with one to one AV conduction, may trigger ventricular fibrillation, as it occurs in the Wolff-Parkinson-White syndrome.

In Wolff-Parkinson-White syndrome, an aberrant working myocardium (“Kent fascicle”) joins

directly the atria to the ventricles out of the specialised AV junction (Fig. 4.27) [57, 58].

Such myocardial bridges between atrial and ventricular myocardium, accessory to the normal AV conducting tissue, have been reported either in structurally normal hearts or in hearts with congenital heart diseases, like Ebstein’s anomaly and congenitally corrected transposition [59]. This aberrant fascicle of working myocardium can be located all around the left and right AV rings, with the exception of the mitro-aortic fibrous continuity area. Accessory pathways in the septal area are less common and are located primarily on the right side. The “Kent fascicle” usually consists of a thin



FIGURE 4–24. Iatrogenic AV block complicating surgical closure of a perimembranous septal defect. (a) Gross view of the cardiac specimen with the septal patch: note the stitches in the postero-inferior rim.

(b) At histology, the surgical stitches cut the AV bundle accounting for AV block (Heidenhain trichrome)

(mean 300 μm in thickness) bundle of working myocardium and, as such, does not possess decremental conduction properties. It may serve not only as bypass tract for ventricular preexcitation (thus explaining the short PQ interval and the delta wave of the QRS) but also as a limb for an AV reentry circuit, which accounts for a reciprocating supraventricular tachycardia, typical of Wolff-Parkinson-White syndrome. Impedance mismatch between the tiny anomalous fibers and the ventricular muscle bulk, in addition to fibrosis of the accessory fascicle, may explain impaired antegrade conduction and intermittent preexcitation. Preexcitation syndromes are a not

so minor cause of sudden death [58–60]. The mechanism is believed to be paroxysmal atrial fibrillation, with one to one conduction, which may degenerate into ventricular fibrillation and cardiac arrest. In these conditions, atrial myocarditis may trigger the onset of life-threatening lone atrial fibrillation [58]. The accessory fascicle along the AV sulcus is always located closer to the endocardium than to the epicardium; size and site are such that “Kent’s fascicle” is easily amenable to endocardial transcatheter ablation, which is the current procedure to interrupt the preexcitation and to reestablish the sole regular electrical connection through the His bundle.

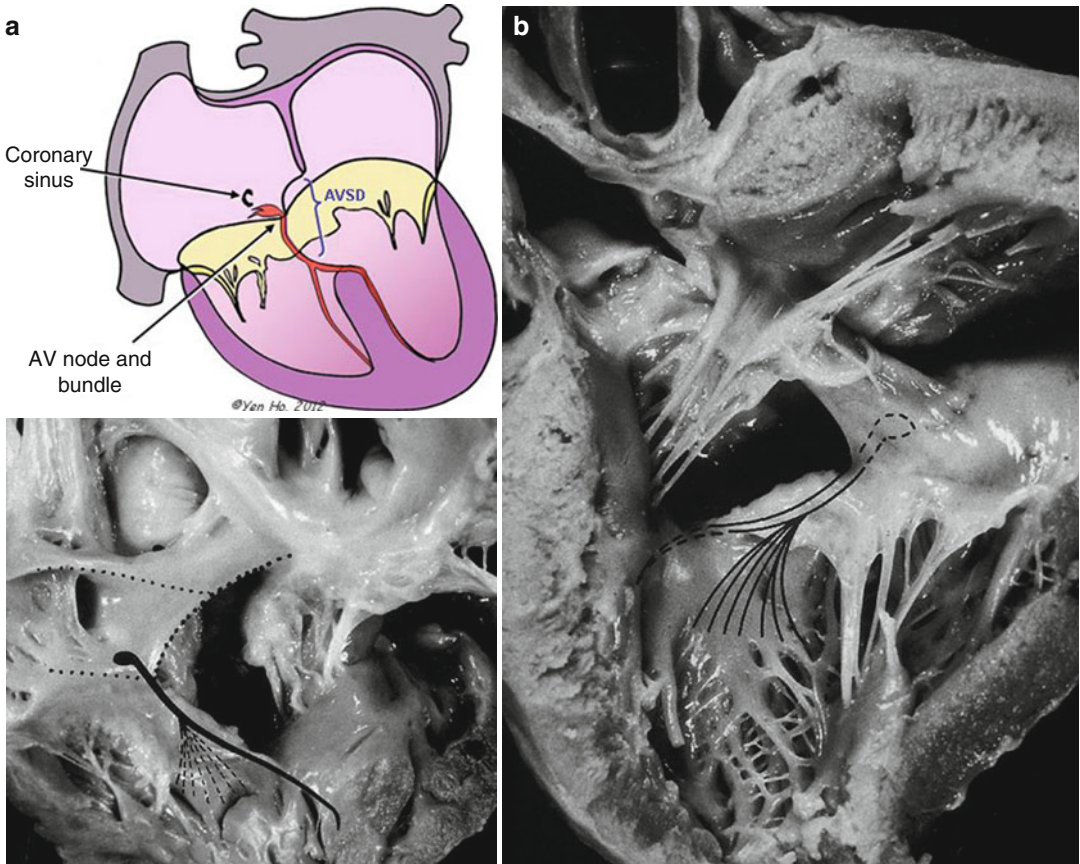


FIGURE 4–25. Conduction system in complete AV canal. (a) Diagram showing the course of the AV axis (AVSD AV septal defect). (b) Gross views of the anatomical specimen showing the location of the AV node and bundle in relationship to the AV septal defect, seen from the left side

Purkinje Cell Tumour (Also Called Histiocytoid Cardiomyopathy, Idiopathic Infantile Cardiomyopathy, Purkinjoma)

This tumour is a rare cause of severe and intractable tachyarrhythmias early in infancy as to be mostly diagnosed at post-mortem [61–63]. It is currently considered a hamartoma arising from the cardiomyocyte or the Purkinje cell, while others consider it as a peculiar type of mitochondrial cardiomyopathy. Macroscopically, these masses present as focal yellowish nodules or areas of discoloration composed of vacuolated

histiocyte-like cells within the myocardium. Their size varies from 1 mm to 1.5 cm in diameter. The most common locations are conduction system and the left ventricle, but they may be also found in the right atrium and ventricle, mostly in the subendocardial layer. Microscopically, these masses contain large oval cardiac myocytes with a coarse granular pale cytoplasm (Fig. 4.28). The cytoplasm is filled with bizarre looking mitochondria. The term oncocytic cardiomyopathy describes the process of the granules (mitochondria) replacing the working myofibrils.

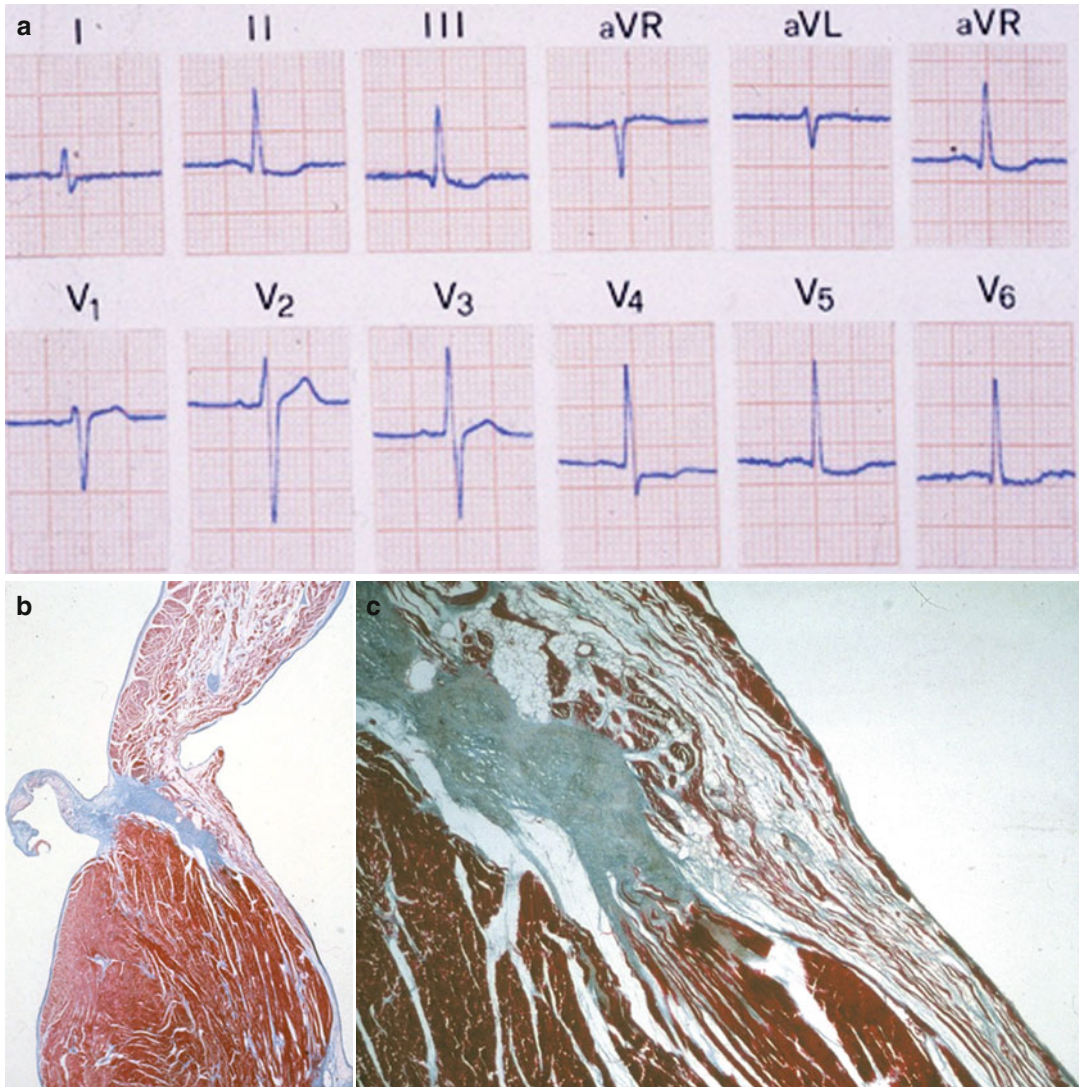


FIGURE 4–26. Lown-Ganong-Levine syndrome. (a) 12 lead ECG tracing with short PR interval and normal QRS complex; (b) extremely hypoplastic AV node (Heidenhain trichrome $\times 6$); (c) close-up of B (Heidenhain trichrome $\times 15$)

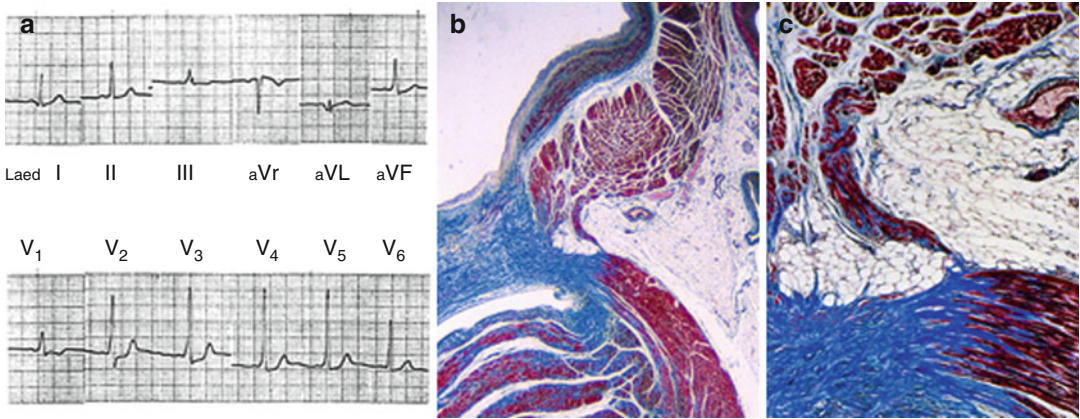


FIGURE 4-27. Wolff-Parkinson-White syndrome. (a) 12 lead ECG tracing with intermittent short PR interval and delta wave; (b) the Kent fascicle, located close to the endocardium, joins the working atrial and

ventricular myocardium (Heidenhain trichrome $\times 6$); (c) close-up of B, with mild fibrosis of the accessory bundle (Heidenhain trichrome $\times 18$)

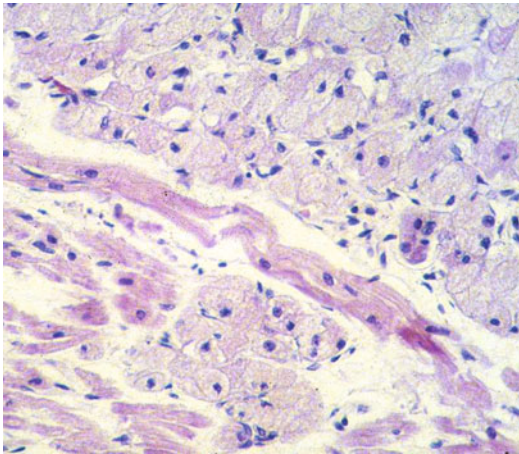


FIGURE 4-28. Purkinje cell tumor in a child who died suddenly. Histology shows focal islands of Purkinje-like cells, clearly distinct from the normal surrounding cardiomyocytes (Hematoxylin-Eosin stain)

References

1. Keith A, Flack M. The form and nature of the muscular connections between the primary divisions of the vertebrate heart. *J Anat Physiol.* 1907;41:172-89.
2. Koch W. *Der funktionelle Bau des menschlichen Herzens.* Berlin: Urban und Schwarzenburg; 1922. p. 92.
3. James TN. Anatomy of the human sinus node. *Anat Rec.* 1961;141:109-16.
4. Truex RC, Smythe MQ, Taylor MJ. Reconstruction of the human sinuatrial node. *Anat Rec.* 1967; 159:371-8.
5. Lev M, Bharati S. Lesions of the conduction system and their functional significance. *Pathol Annu.* 1974;8:157-60.
6. Hudson REB. The human pacemaker and its pathology. *Br Heart J.* 1960;22:153-6.
7. Anderson KR, Ho SY, Anderson RH. Location and vascular supply of sinus node in human heart. *Br Heart J.* 1979;41:28-32.
8. Sanchez-Quintana D, Cabrera C, Farre J, Climent V, Anderson RH, Ho SY. Sinus node revisited in the era of electroanatomical mapping and catheter ablation. *Heart.* 2005;91:189-94.
9. Busquet J, Fontan E, Anderson RH, Ho SY, Davies MJ. The surgical significance of the atrial branches of the coronary arteries. *Int J Cardiol.* 1984;6:223-34.
10. James TN. Structure and function of the sinus node, AV node and His bundle of the human heart: part I-structure. *Prog Cardiovasc Dis.* 2002;45:235-67.
11. James TN. The internodal pathways of the human heart. *Prog Cardiovasc Dis.* 2001;43:495-535.
12. Tawara S. *Das Reizleitungssystem des Säugetierherzens.* Jena: Gustav Fischer; 1906.
13. Olgin JE, Ursell PC, Kao AK, et al. Pathological findings following slow pathway ablation for AV nodal reentrant tachycardia. *J Cardiovasc Electrophysiol.* 1996;7:625-31.
14. Ho SY, Anderson RH. How constant anatomically is the tendon of Todaro as a marker of the triangle of Koch? *J Cardiovasc Electrophysiol.* 2000;11:83-9.
15. His W. Die thatigkeit des embryonalen herzens und deren bedeutung fur die lehre von der herzbewegung beim erwachsenen. *Med Klin Leipzig.* 1893;1:14-49.

16. Sanchez-Quintana D, Ho SY, Cabrera JA, Farre J, Anderson RH. Topographic anatomy of the inferior pyramidal space: relevance to radiofrequency ablation. *J Cardiovasc Electrophysiol*. 2001;12:210–7.
17. Kurosawa H, Becker AE. Dead-end tract of the conduction axis. *Int J Cardiol*. 1985;7:13–8.
18. Inoue S, Becker AE. Posterior extensions of the human compact AV node. A neglected anatomic feature of potential clinical significance. *Circulation*. 1998;97:188–93.
19. Ho SY, McCarthy KP, Ansari A, Thomas PS, Sanchez-Quintana D. Anatomy of the atrioventricular node and atrioventricular conduction system. *J Bifurcation Chaos*. 2003;12:3665–74.
20. Pieperhoff S, Borrmann C, Grund C, Barth M, Rizzo S, Franke WW. The area composita of adhering junctions connecting heart muscle cells of vertebrates. VII. The different types of lateral junctions between the special cardiomyocytes of the conduction system of ovine and bovine hearts. *Eur J Cell Biol*. 2010;89:365–78.
21. Rossi L, editor. *Histopathology of cardiac arrhythmias*. Philadelphia: Lea & Febiger; 1979.
22. Rossi L, Thiene G. *Arrhythmologic pathology of sudden cardiac death*. Milano: Casa Editrice Ambrosiana; 1983.
23. Davies MJ. *Pathology of conducting tissue of the heart*. London: Butterworths; 1971.
24. Thiene G, Valente M, Rossi L. Involvement of the cardiac conducting system in panarteritis nodosa. *Am Heart J*. 1978;95:716–24.
25. Marinato PG, Thiene G, Menghetti L, Buja GF, Nava A, Cecchetto A, et al. Clinicopathologic assessment of arrhythmias in a case of scleroderma heart disease with sudden death. *Eur J Cardiol*. 1981;12:321–31.
26. Calzolari V, Angelini A, Basso C, Livi U, Rossi L, Thiene G. Histologic findings in the conduction system after cardiac transplantation and correlation with electrocardiographic findings. *Am J Cardiol*. 1999;84:756–9.
27. Davies MJ. Pathology of chronic A-V block. *Acta Cardiol*. 1976;21:19–30.
28. Mahaim I. *Maladies organiques du faisceau de His-Tawara*. Paris: Masson et Cie; 1931.
29. Bharati S. Pathology of the conduction system. In: Silver MD, Gotlieb AI, Schoen FJ, editors. *Cardiovascular pathology*. 3rd ed. Philadelphia: Churchill Livingstone; 2001. p. 607–28.
30. Chameides L, Truex RC, Vetter V, Rashkind WJ, Galioto Jr FM, Noonan JA. Association of maternal systemic lupus erythematosus with congenital complete heart block. *N Engl J Med*. 1977;297:1204–7.
31. Angelini A, Moreolo GS, Ruffatti A, Milanese O, Thiene G. Calcification of the atrioventricular node in a fetus affected by congenital complete heart block. *Circulation*. 2002;105:1254–5.
32. Becker AE, Lie KI, Anderson RH. Bundle-branch block in the setting of acute anteroseptal myocardial infarction. Clinicopathological correlation. *Br Heart J*. 1978;40:773–82.
33. James TN. De subitaneis mortibus. XXIII. Rheumatoid arthritis and ankylosing spondylitis. *Circulation*. 1977;55:669–77.
34. Nguyen HH, Wolfe 3rd JT, Holmes Jr DR, Edwards WD. Pathology of the cardiac conduction system in myotonic dystrophy: a study of 12 cases. *J Am Coll Cardiol*. 1988;11:662–71.
35. Lev M. Anatomic basis for atrio-ventricular block. *Am J Med*. 1964;37:742–8.
36. Lenegre J, Moreau P. Chronic auriculo-ventricular block. Anatomical, clinical and histological study. *Arch Mal Coeur Vaiss*. 1963;56:867–88.
37. Maron BJ, Towbin JA, Thiene G, Antzelevitch C, Corrado D, Arnett D, et al. Contemporary definitions and classification of the cardiomyopathies. An American Heart Association Scientific Statement from the Council on Clinical Cardiology, Heart Failure and Transplantation Committee; Quality of care and outcomes research and functional genomics and translational biology interdisciplinary working groups, and council on epidemiology and prevention. *Circulation*. 2006;113:1807–16.
38. Schott JJ, Alshinawi C, Kyndt F, Probst V, Hoorntje TM, Hulsbeek M, et al. Cardiac conduction defects associate with mutations in SCN5A. *Nat Genet*. 1999;23:20–1.
39. James TN. Clinicopathologic correlations. De subitaneis mortibus. XXV. Sarcoid heart disease. *Circulation*. 1977;56:320–6.
40. Thiene G, Rossi L, Becker AE. The atrioventricular conduction system in dissecting aneurysm of the aorta. *Am Heart J*. 1979;98:447–52.
41. James TN, Galakhov I. De subitaneis mortibus. XXVI. Fatal electrical instability of the heart associated with benign congenital polycystic tumor of the atrioventricular node. *Circulation*. 1977;56:667–78.
42. Basso C, Valente M, Poletti A, Casarotto D, Thiene G. Surgical pathology of primary cardiac and pericardial tumors. *Eur J Cardiothorac Surg*. 1997;12:730–7.
43. Thiene G, Miraglia G, Menghetti L, Nava A, Rossi L. Multiple lesions of the conduction system in a case of cardiac rhabdomyosarcoma with complex arrhythmias. An anatomic and clinical study. *Chest*. 1976;70:378–81.
44. Fraccaro C, Buja G, Tarantini G, Gasparetto V, Leoni L, Razzolini R, et al. Incidence, predictors,

- and outcome of conduction disorders after transcatheter self-expandable aortic valve implantation. *Am J Cardiol.* 2011;107:747–54.
45. Farré J, Cabrera JA, Sánchez-Quintana D, Ho SY, Anderson RH. Anatomy of the atria for rhythmologists. *Arch Mal Coeur Vaiss.* 2003;96(Spec No 7):32–6.
 46. Critelli G, Gallagher JJ, Thiene G, Perticone F, Monda V, Rossi L. Histologic observations after closed chest ablation of the atrioventricular conduction system. *JAMA.* 1984;252:2604–6.
 47. Ho SY, Seo JW, Brown NA, Cook AC, Fagg NL, Anderson RH. Morphology of the sinus node in human and mouse hearts with isomerism of the atrial appendages. *Br Heart J.* 1995;74:437–42.
 48. Rossi L, Montella S, Frescura C, Thiene G. Congenital atrioventricular block in right atrial isomerism (asplenia). A case due to atrionodal discontinuity. *Chest.* 1984;85:578–80.
 49. Daliento L, Corrado D, Buja G, John N, Nava A, Thiene G. Rhythm and conduction disturbances in isolated, congenitally corrected transposition of the great arteries. *Am J Cardiol.* 1986;58:314–8.
 50. Thiene G, Nava A, Rossi L. The conduction system in corrected transposition with situs inversus. *Eur J Cardiol.* 1977;6:57–70.
 51. Anderson RH, Ho SY, Becker AE. The surgical anatomy of the conduction tissues. *Thorax.* 1983;38:408–20.
 52. Thiene G, Wenink AC, Frescura C, Wilkinson JL, Gallucci V, Ho SY, et al. Surgical anatomy and pathology of the conduction tissues in atrioventricular defects. *J Thorac Cardiovasc Surg.* 1981;82:928–37.
 53. Daliento L, Nava A, Fasoli G, Mazzucco A, Thiene G. Dysplasia of the atrioventricular valves associated with conduction system anomalies. *Br Heart J.* 1984;51:243–51.
 54. Anderson RH, Becker AE, Brechenmacher C, Davies MJ, Rossi L. Ventricular preexcitation. A proposed nomenclature for its substrates. *Eur J Cardiol.* 1975;3:27–36.
 55. Lown B, Ganong WF, Levine SA. The syndrome of short P-R interval, normal QRS complex and paroxysmal rapid heart action. *Circulation.* 1952;5:693–706.
 56. Ometto R, Thiene G, Corrado D, Vincenzi M, Rossi L. Enhanced A-V nodal conduction (Lown-Ganong-Levine syndrome) by congenitally hypoplastic A-V node. *Eur Heart J.* 1992;13:1579–84.
 57. Becker AE, Anderson RH, Durrer D, Wellens HJ. The anatomical substrates of Wolff-Parkinson-White syndrome. A clinicopathologic correlation in seven patients. *Circulation.* 1978;57:870–9.
 58. Basso C, Corrado D, Rossi L, Thiene G. Ventricular preexcitation in children and young adults: atrial myocarditis as a possible trigger of sudden death. *Circulation.* 2001;103:269–75.
 59. Thiene G, Pennelli N, Rossi L. Cardiac conduction system abnormalities as a possible cause of sudden death in young athletes. *Hum Pathol.* 1983;14:704–9.
 60. Basso C, Frescura C, Corrado D, Muriago M, Angelini A, Daliento L, et al. Congenital heart disease and sudden death in the young. *Hum Pathol.* 1995;26:1065–72.
 61. James TN, Beeson 2nd CW, Sherman EB, Mowry RW. Clinical conference: De subitaneis mortibus. XIII. Multifocal Purkinje cell tumors of the heart. *Circulation.* 1975;52:333–44.
 62. Malhotra V, Ferrans VJ, Virmani R. Infantile histiocytoid cardiomyopathy: three cases and literature review. *Am Heart J.* 1994;128:1009–21.
 63. Ottaviani G, Matturri L, Rossi L, Lavezzi AM, James TN. Multifocal cardiac Purkinje cell tumor in infancy. *Europace.* 2004;6:138–41.